A Simulated Amphibious Salamander Robot: Exploration of the Morphological Configuration and the Locomotion Controller

Jérôme Braure, Olivier Michel, Alessandro Crespi, and Auke Jan Ijspeert

***Abstract*— This article describes the development of a software model of an amphibious salamander robot. The robot is characterized by a spine with multiple degrees of freedom and by four rotating legs. The simulated robot is capable of three different types of locomotion, namely swimming, crawling, and walking. It represents a realistic model of a real robot called *AmphiBot II* currently under assembly. The model is created with the physics-based mobile robot simulator *Webots*. In this article, numerical experiments are carried out to characterize the influence of different morphology and controller parameters on the velocity of the three types of locomotion.**

The experiments identify the optimal leg shapes for fast walking. They also identify which types of spine undulations are optimal for the three modes of locomotion. In particular, it is found that a stationary undulation of the spine can increase walking speeds by a factor of three compared to rigid spines. It is also found that the travelling undulations for fastest locomotion are significantly different (in terms of amplitude and wavelength) between crawling on ground and swimming in water.

***Index Terms*— Mobile robotics, amphibious robots, simulation, articulated rigid body dynamics, salamander, legged locomotion, serpentine locomotion, swimming.**

I. Introduction

THE TASKS entrusted to robots are becoming increasingly varied and numerous. Programming an automaton to perform a given predefined movement can be fairly easy, whereas creating a robot that is autonomous and able to adapt itself to different kinds of environments is a completely different problem. One of the most concerned features is locomotion. In this field, it is obvious that even simple animals are nimbler than the most high-tech existing robot. Moreover, it has been proved many times in the past century that taking inspiration from Nature for scientific and engineering purposes can yield great benefits.

We are currently in the process of building an amphibious robot that is inspired by the salamander. The robot's snake-like version is named *AmphiBot I* [1], [2] and the legged version is called *AmphiBot II*. The goal of the project is three-fold: (1) to construct a robot that replicates the salamander's ability to move in a large array of aquatic and semi-aquatic environments, (2) to develop novel ways of adaptively controlling locomotion in robots with multiple degrees of freedom using systems of coupled nonlinear oscillators, and (3) to test neurobiological models of the salamander locomotor system.

The salamander was chosen because of the diversity of locomotion types that it uses, namely swimming, crawling and walking, and its interesting features from a neurobiological point of view. The salamander indeed represents, among vertebrates, a key animal in the evolution of legged locomotion. Thus, studying the salamander's locomotion control mechanisms will eventually improve the understanding of motor control mechanisms in higher vertebrates, including humans.

The robot will replicate the salamander's features, in particular its flexible spine, and its different modes of locomotion. It will be used to perform exploration and inspection tasks in a variety of environments, and will serve as a test-bench for experimenting adaptive control of locomotion.

The goals of this research are to develop a realistic virtual model of the salamander robot in a physics-based simulator, and to use it to analyze how morphological and control considerations affect the different modes of locomotion of the robot. In a first study, we use the simulator to explore different design options of the legs, in order to identify those that optimize speed and stability of walking. In a second study, we identify which undulations (in terms of frequency, wavelength and amplitude of travelling waves) optimize the speed of swimming, crawling, and walking. These studies are realized by performing systematic searches in the morphological and control parameter spaces (see Section V).

Some of the questions that we address are: Do body undulations increase the velocity during legged locomotion? What is the influence of the legs shapes on the robot's speed and stability? What is the optimal body wavelength for a snake? And the optimal oscillation frequency and amplitude? Do these optimal settings remain the same when the snake transits from ground to water? How does the transversal to longitudinal friction ratio affect the speed in serpentine locomotion?

The usage of a simulator has many advantages: it can accelerate the development process and experiments can be performed without risking any material damage (real robots can be quite expensive, especially prototypes). Different scenarios can be tested using exactly identical initial conditions and the simulation allows a broader variety of test-runs than the real robot does. Physical features can be dynamically modified without having to mechanically rebuild a piece.

Manuscript received month XX, 200X; revised month XX, 200X.
J. Braure (email: jerome.braure@a3.epfl.ch)
O. Michel (email: olivier.michel@cyberbotics.com)
A. Crespi (email: alessandro.crespi@epfl.ch)
A.J. Ijspeert (email: auke.ijspeert@epfl.ch)
Acknowledgments: This work was funded by the Swiss National Science Foundation (Young Professorship award 620 - 066143 to A.J. Ijspeert), and by the Swiss Federal Office for Professional Education and Technology (Technology Transfer CTI, project 6395.1 ENS-ET).
Correspondence to A.J. Ijspeert.

Various kinds of data can be easily output or plotted. This work will also provide a good idea of how close to reality a simulator can be, thus allowing us to bring enhancements to the simulator.

In section II we will first provide a literature review regarding the robots that are related to our field of study. Then, we will describe the design considerations underlying the real robots (section III) and the implementation of our salamander robot model in the simulator (section IV). Experimental runs will be conducted and their results analyzed (section V) and discussed (section VI). The article ends with a review of future work (section VII) and a conclusion (section VIII).

II. Literature review

Many different biologically inspired robots have already been built. Some of them try to resemble as much as possible to a particular kind of animal while others only use certain features like the morphology of a leg or a type of gait.

The following (non-exhaustive) list describes some existing robots, using quadrupedal, serpentine or aquatic locomotion.

A. Bio-inspired robots

1) Quadrupeds: The first computer controlled walking machine, the quadruped named Phoney Poney, was built in 1966 at the University of South Carolina. A large array of quadruped robots have since been built [3], [4], [5]. Recently, robots featuring an articulated spine have appeared, three of them replicating the sprawling posture of the salamander [6], [7], [8]. These robots allow one to investigate how an articulated spine can help increase the velocity and agility (e.g. the ability to turn) of a quadruped robot. But, to date, no detailed and quantitative analysis of the benefits of an articulated spine have been published.

2) Snake robots: Snake-like robots appeared as early as the 70's [9]. Snakes present different modes of locomotion, including serpentine locomotion (or lateral undulation), sidewinding, concertina locomotion, and rectilinear locomotion. Most snake robots use serpentine locomotion in which a lateral undulation is propagated as a travelling wave from head to tail. The differential friction required for the serpentine locomotion is often recreated by simply fixing little passive wheels at the bottom of each segment of the body. Remote controlled snakes performing a very realistic serpentine movement, including sidewinding, were built in the nineties [10]. Other types of snake robots can be found in [11], [12].

3) Eel robots: Eel-like or lamprey-like robots have the characteristic of using their entire body to provide thrust, in an aquatic environment. Two interesting examples include a lamprey-like robot actuated by shape-memory alloys [13], and an amphibious eel robot actuated by servo motors that is able to swim and to crawl on the ground using four distinct gaits and their reverse motion [14].

4) Fish robots: Several fish robots have been created, some of them shaped like a tuna, with a flexible hull and an oscillating foil [15], [16]. Experiments have demonstrated a great autonomy, good performances and large payload capacities, better than existing autonomous undersea vehicles. One of the experimental results obtained was that the drag of the swimming tuna robot appeared to be less than the drag on the straight body.

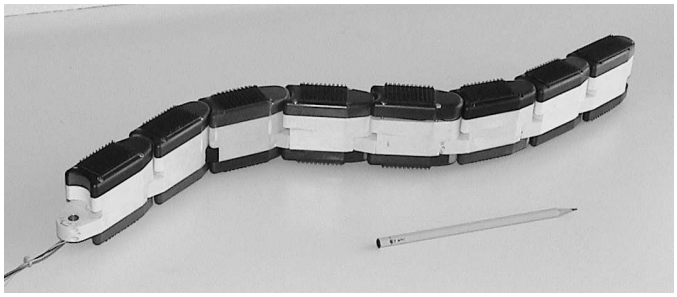

Fig. 1. AmphiBot I (Snake configuration).

5) Amphibious robots: Several waterproof legged robots have been created. Some of them [17] have the ability to transit from ground to water and inversely. Others were specifically designed for underwater walking [18]. In addition to the eel robots mentioned above, an amphibious snake-like robot has been created, able to both swim in water and crawl with serpentine locomotion on the ground [19].

To the best of our knowledge, there is currently no robot capable of walking, crawling and swimming, and this constitutes one of the challenges that we aim to tackle with our *AmphiBot II* robot.

B. The salamander's locomotion

The salamander exhibits three types of locomotion: walking, crawling and swimming. For walking, an S-shaped standing wave is induced in the body with two nodes corresponding to the locations where the front/rear legs are attached to the body [20]. The undulation of the body is coordinated with the legs' motion in order to optimize the legs' reach during swing phase. The phase relation between the legs' motion is the same as that of the trot. For crawling and swimming, the legs are not used and are maintained along the body. In these cases, a travelling wave is induced along the body, propagating from head to tail [20]. Crawling is only used as an 'emergency' gait, to escape from a danger as it produces a higher velocity.

In previous works, we developed a connectionist central pattern generator (CPG) model for the aquatic and terrestrial gaits of a simulated salamander [21]. That work aimed at investigating the neural mechanisms underlying gait generation and gait transition in the salamander. One of the purposes of the real robot under construction is to serve as a validation test-bed for those neural models.

III. Design considerations of the real robots

Our robots are of two types: Amphibot I which is an amphibious snake robot (see figure 1), and Amphibot II (currently under construction) which is the salamander robot and corresponds to Amphibot I with two additional leg elements (one for the fore-limbs and one for the hind-limbs). The robots are designed to present the following characteristics:

- Modularity. We aim at having a robot that is composed of multiple identical spine elements (see figure 2). This

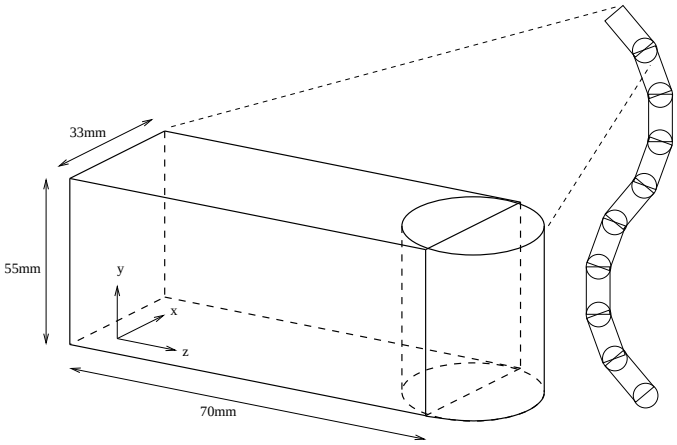

Fig. 2. AmphiBot body segment and top view of the robot body.

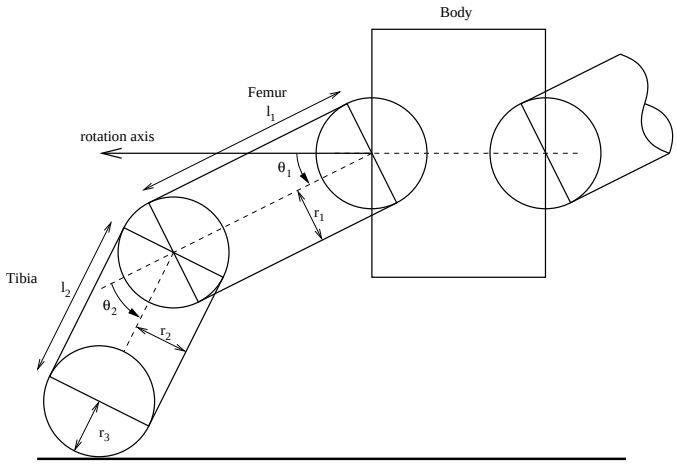

Fig. 3. Leg morphology. The rectangle represents the front of a body segment. The radii r_1, r_2 and r_3 are usually equal unless explicitly specified.

allows us to quickly adjust the length of the robot by adding or removing elements.

- To have distributed actuation, power and control. In order to be truly modular, each element carries its own DC motor, battery, and micro-controller.
- To be waterproof. Each individual element is made waterproof (as opposed to having a coating covering a chain of elements). This facilitates modularity and ensures that a leakage will only damage a single element.
- To be slightly buoyant. We aim at having a robot that passively returns to the surface of the water when inactive. Furthermore, we construct the elements such that the center of gravity is placed below the geometrical center, in order to obtain a vertical orientation that self-stabilizes in water.
- To have large lateral surfaces for good swimming efficiency.
- To have asymmetric friction for serpentine locomotion (lower friction coefficient in the longitudinal axis compared to the perpendicular axis).
- To be controlled by a CPG composed of coupled nonlinear oscillators.
- To be remotely controlled in terms of speed and direction commands, but otherwise have an on-board locomotion controller for coordinating its multiple degrees of freedom.
- To have one-DOF legs (see figures 3 and 4) used for propulsion on ground and for steering in water (AmphiBot II).

The construction details are provided in [1], [2].

IV. Software model implementation

This article presents the software models of the snake and salamander robots. The implementation of the robot models is done in the mobile robot simulator *Webots* [22], see figure 4. Webots is using the Open Dynamics Engine (ODE) library [23] to simulate articulated rigid body dynamics.

A. Robot body

The spine is composed of several identical segments. One of these segments is depicted on figure 2.

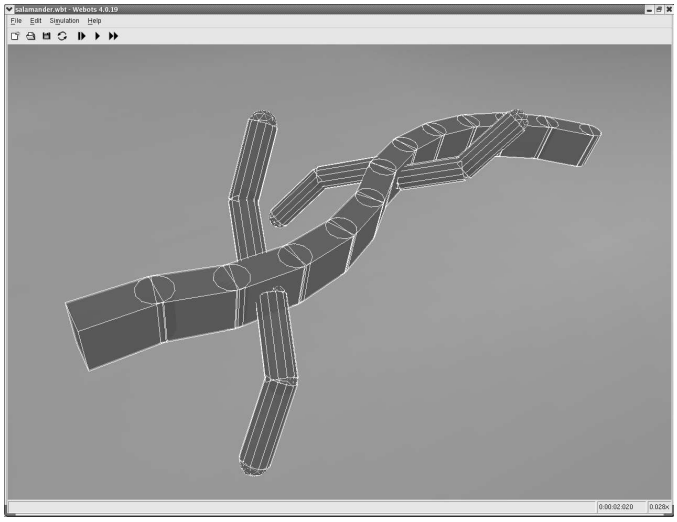

Fig. 4. Model of AmphiBot II in Webots.

In the Webots world description file, each body segment is a servo object shaped by a box and a cylinder. The legs are made up of two cylinders (femur and tibia) plus three spheres (hip, knee and foot) at the junctions, all contained in a servo. There are two other servos embedded in the leg (one for the hip and one for the knee), but they are not actuated. They are needed for setting the limb geometry, and could simulate a leg bending under compression, however in present implementation the legs are made stiff. We call them *legs* but they are actually wheel-legs (sometimes called whegs). Since salamanders have *legs*, we will keep that denomination.

In the current implementation, collisions between limbs and body parts have been deactivated (i.e. two legs cannot collide, they just 'pass' through each other, the same happens for body segments) in order to avoid any influence or 'special' behavior taking advantage of these collisions to produce a type of locomotion. This is clearly a simplification, but the gaits tested in this article do not produce inter-segment collisions except in a few particular cases (see SectionV).

B. Motor control

The real robot Amphibot I is powered by 0.75W DC motors and controlled by PD position controllers that use magnetic encoders on the motor axis to provide a feedback signal [2]. We simulate such a motor and its control loop using a servo element in Webots. The servo uses an *Angular Motor* provided by ODE. An Angular Motor allows one to apply a desired angular velocity to an actuated joint. Unlike a PID controller, the desired angular velocity is set in a single time step, provided that this does not take more torque than is allowed by a maximum torque parameter. ODE does this by using the desired angular velocity as a constraint, and effectively computing one time step into the future to work out the correct torque.

The PD position controller of the real robot is therefore simulated by the following feedback control loop: $\omega = k(\bar{\theta} - \theta)$, where ω is the angular velocity applied to the joint, k is a positive gain, $\bar{\theta}$ is the desired angle, and θ is the actual angle.

C. Trajectory generator

In this article, the locomotion controller is a simple sine trajectory generator, i.e. an 'open-loop' controller that sends desired positions to the servos, without sensory feedback. It is only used for characterization of legged, swimming or serpentine locomotion (crawling). As a convention, the fist spine-servo, between the head segment and the second segment is denoted servo_1 (following servos are numbered increasingly) and the legs are designated as leg 1, 2, 3 and 4 which respectively corresponds to front left, front right, rear left and rear right leg.

1) Swimming and crawling: In this case, the body undulates with a travelling wave, propagating from head to tail. The angle $\alpha_i(t)$ of spine servo i at time t is computed according to the following expression:

$$\alpha_i(t) = A \cdot \sin\left(2\pi\nu t - \frac{2\pi i}{\lambda}\right) \tag{1}$$

where A is the peak amplitude, λ is the wavelength expressed in multiples of the segment length and ν the frequency. The leg servo angle $\gamma_i(t)$ for leg i follows:

$$\gamma_i(t) = 3\pi/2 \qquad i = 1, 2, 3, 4 \tag{2}$$

At a servo angle of $\gamma_i(t) = 0$ the leg is in an upright position and at $\gamma_i(t) = 3\pi/2$ the legs are simply maintained backwards, along the body.

2) Walking: We use the term *walking*, but technically, it corresponds to the phase relation of a trotting gait. In this case, the body is separated into three parts (neck, trunk and tail) which all oscillate as a standing wave with a phase shift of π between two contiguous parts. The parts' boundaries are defined as the locations where the legs are connected to the body. The spine servos' angles are thus:

$$\alpha_i(t) = \begin{cases} A \cdot \sin(2\pi\nu t) & \text{if } \mathrm{servo}_i \in \mathrm{neck, tail} \\ A \cdot \sin(2\pi\nu t + \pi) & \text{if } \mathrm{servo}_i \in \mathrm{trunk} \end{cases} \tag{3}$$

And the legs' servo angles are:

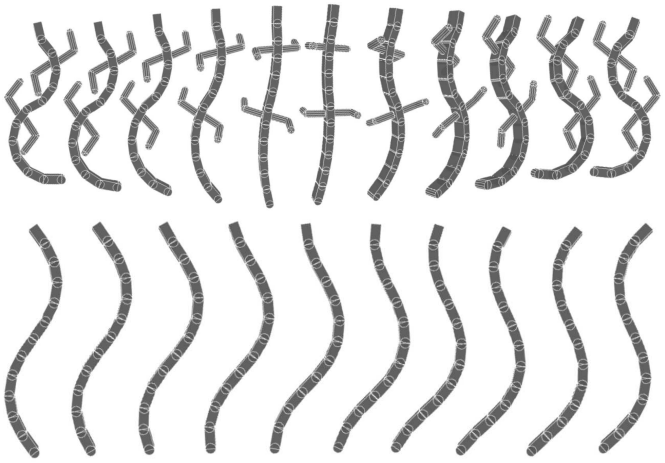

Fig. 5. Sequence of the AmphiBot I/II model walking and swimming/crawling (half periods).

$$\gamma_i(t) = \begin{cases} \omega t & \text{if } i = 1, 4 \\ \omega t + \pi & \text{if } i = 2, 3 \end{cases} \tag{4}$$

Where ω is the angular velocity, equal to $2\pi\nu$ rad/s for the experiments presented in this article.

Figure 5 shows the movements of the AmphiBot I/II model walking and crawling.

D. Physics

ODE (Open Dynamics Engine [23]), upon which Webots is built, takes care of the physical interactions between the bodies in our simulated world. ODE's function library are used to create rigid bodies (solid objects), joints (between the objects), simulate the dynamics and to detect and handle collisions.

1) Hydrodynamics: Neither ODE nor Webots have the notion of 'water'. Therefore, to be able to create a swimming salamander, custom-made external forces have to be applied on the robot to simulate the effect of water. These are (a) the force due to Archimedes' principle and (b) the drag.

a) Archimedes' Principle: Definition: *When a body is wholly or partly immersed in a fluid, it experiences an upthrust or buoyant force equal to the weight of fluid it displaces.*

This force, usually denoted as Archimedes' force is computed using the following expression, which comes from the definition.

$$\vec{F_A} = -V_{body} \cdot \rho_{fluid} \cdot \vec{g}$$

Where V_{body} is the volume of the immersed body, ρ_{fluid} is the fluid's density and $\vec{g}$, the gravitational force vector. One must notice that this force does not depend on the depth. Archimedes' force is computed independently for each segment of the body, including the legs.

The body's density is usually set to the same density as the fluid (in our case: water) to assure neutral buoyancy during underwater test runs. A density lower than the water density will give the robot the characteristics of a floating body.

b) Drag: The drag force is complex to compute, since it involves computing fluid dynamics around a deformable body. In our simulation, we simplify the computation by assuming that the speed of the water relative to the body is sufficiently high for the forces exerted by the water to be mainly inertial forces (high Reynolds number). It is also assumed that the water is stationary and that the parallel and perpendicular components of the force exerted by the water on each link can be calculated separately.

The drag forces are therefore computed as follows:

$$F_{D_i} = \frac{1}{2} \cdot \rho_{water} \cdot S_i \cdot C_i \cdot v_i^2 \qquad i = x, y, z$$

F_{D_i} is the force to be applied along the body's i axis, where S_i is the body's section (surface) perpendicular to the axis, C_i is the drag coefficient relative to the i axis, and v_i the component of the body's velocity on its i axis. At each time-step and for each segment, the three components of the drag force are computed separately and applied to the body. The drag coefficients, usually denoted C_D in textbooks, are in our case only a rough approximation of the reality, the computation of their precise values would be very complex. Fluids mechanics literature [24] provides the C_D's of various bodies, depending on their dimensions and shapes. The salamander body segments are approximated (for the x and y axes) as two-dimensional[1] bodies, since the flow is blocked at both extremities by the neighboring segment.

2) Friction: ODE takes care of the friction at contact points using the Coulomb friction model. The friction force is determined by a coefficient friction parameter μ. When the tangential external force $|f_T|$ applied to the object is smaller or equal to $\mu \cdot |f_N|$ (where $|f_N|$ is the normal force), the contact is static and the friction force $|f_F|$ exactly opposes the tangential external forces (i.e. $|f_F|$= $|f_T|$). If it is not the case, the contact is dynamic, and the friction force is proportional to the normal force, $|f_F| = \mu \cdot |f_N|$, and opposed to the direction of motion. Different friction coefficients can be set for the two different axis defining the contact surface. If not stated otherwise, $\mu = 0.4$ for the body-ground and foot-ground contacts.

E. Automated Body Synthesis

A program needed to generate a robot with custom dimensions was then developed, in order to allow batch runs. The features that can be set are: the body length, (i.e. the number of elements constituting the body), the attach position of the legs and various leg characteristics as depicted on figure 3. The orientation of the leg-actuating servo can also be set, by modifying the angles in the horizontal and vertical planes.

The legs are actually optional. A legless salamander (denoted as a *snake* throughout the rest of the article) can thus be generated to simulate AmphiBot I. Some of the physical parameters can also be customized, like for example the body density, the friction constant, and the bounce coefficient.

[1]In terms of fluids mechanics, two-dimensional means that the flow (e.g. water) passes above and under the body, but not around the sides. For instance, a segment within a bar of infinite length perpendicular to the flow is considered as a two-dimensional body.

F. Simulated time vs real time

Webots uses a first order Euler integration with a 30 ms time step. The speed of the simulation depends on the computational load. In our case, the simulated time is about 3 times faster than real time in swimming locomotion, 1.3 times when crawling (the many contacts with the ground require a lot of computation) and 0.7 times for walking (at a time step of 5 ms instead of 30 ms to prevent numerical explosions caused by the sharp peaks in the forces produced when the feet hit the ground).

V. Experimentation

We are now equipped with a fully customizable salamander model which allows us to address the following questions: Do body undulations increase the velocity during legged locomotion? What is the influence of the legs shapes on the robot's speed and stability? What is the optimal body wavelength for a snake? And the optimal oscillation frequency and amplitude? Do these optimal settings remain the same when the snake transits from ground to water? How does the transversal to longitudinal friction ratio affect the speed in serpentine locomotion?

The software model of the salamander has many degrees of freedom and it is therefore not feasible to perform an exhaustive search in order to find the optimal configuration (e.g. in terms of maximum velocity). The search space is not even discrete, it means that the number of different possibilities is infinite. We will therefore search by fixing some of the variables and examine sets of evenly distributed values.

The salamander's parameters can be divided into two categories:

1) The parameters concerning the physical shape, or morphology of our robot.
2) The parameters influencing the movements. These parameters actually define the way the servos are actuated.

A. Robot morphology

In this part we study by which manner the morphology of our salamander, especially the shape of the legs, affects its performances. The result of these experiments will guide the design of AmphiBot II's legs, currently under construction.

The salamanders used for these batch test runs have a length of twelve segments, the front legs are attached to the third segment and the rear legs are connected to the seventh segment, as depicted on figure 4. For each run, which lasts seven seconds, the average speed of the run is computed by dividing the straight line distance between the start and end positions by the duration of the run. The reason why we study the average speed instead of the maximal speed or the final speed is because the instant speed varies too much and too quickly to provide useful and comparable data. Moreover, privileging the instant speed could select an awkward configuration as being the best. For instance a salamander constantly walking in circles with a fast pace would be preferred to a sane individual walking on a straight line with a lower velocity. Thus considering the distance reached after a given amount of time appears to be much more relevant in our case.

TABLE I

EXPERIMENTS ON THE LEGS MORPHOLOGY. VALUES BETWEEN BRACKETS DEFINE THE RANGE AND GRANULARITY OF THE VARYING PARAMETERS: [LOWER-BOUND : STEP : UPPER-BOUND].

Experiment number	l_1 [m]	l_2 [m]	θ_1 [deg]	θ_2 [deg]
1.a	[0.02:0.02:0.1]	[0.02:0.02:0.1]	[0:10:90]	[0:10:90]
1.b	0.08	0.08	[0:10:90]	[0:10:90]
1.c	[0.02:0.02:0.1]	[0.02:0.02:0.1]	30	30

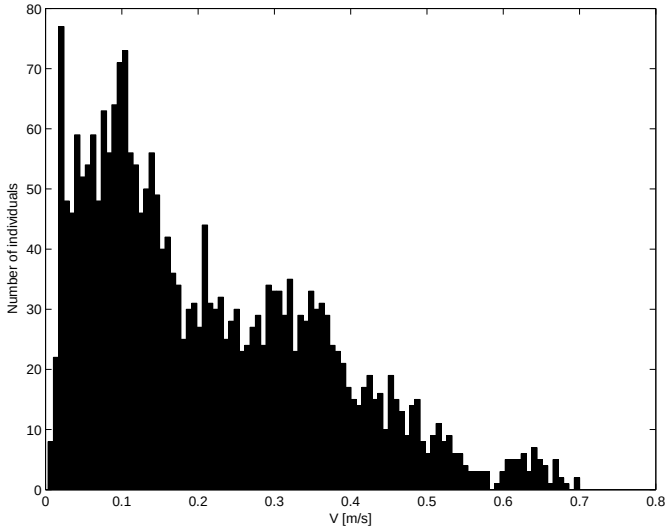

Fig. 6. Experiment 1.a. Histograms showing the distribution of the velocities reached by the differently legged individuals.

Table I gives some details about the fixed and variable parameters in each experiment. The walking trajectories are not varied in this experiment. They are defined by a body servo amplitude set to $A = 25°$ and a frequency $\nu = 1$ Hz.

1) Experiment 1.a: Distribution of velocities for differently legged individuals: The variables tested in this preliminary study are: l_1, l_2, θ_1 and θ_2, respectively the femur and tibia lengths and the femur and tibia angles in the vertical plan.

The results of this first experiment are displayed on figure 6. The cardinality of the set is 2500. The fastest individual, with a velocity of 0.7 m/s has the following leg morphology settings: $\theta_1 = 40°$, $\theta_2 = 0°$ and $l_1 = l_2 = 0.1$ m. That is, this individual uses the longest legs of the set. This configuration places the feet at a maximal distance from the body (to increase the stability) and from the leg rotation axis, thus letting each foot describe a large circle around the axis. The three best configurations are shown on figure 7.

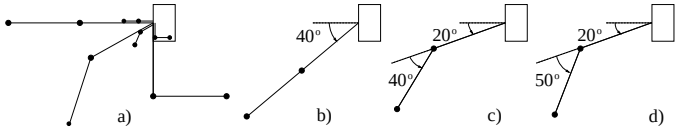

Fig. 7. Front views of leg configurations for experiment 1.a. a) Range of angles and lengths tested: $\theta_1 = \theta_2 = 0°$ to $\theta_1 = \theta_2 = 90°$, $l_1 = l_2 = 0.02$ m to $l_1 = l_2 = 0.1$ m, plus an intermediate position. Leg configuration of b) the fastest, c) the second and d) the third fastest individual of experiment 1.a. All three have $l_1 = l_2 = 0.1$ m.

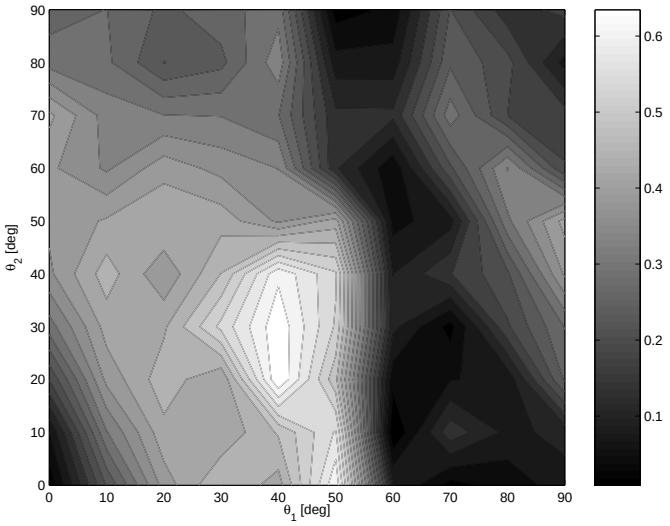

Fig. 8. Experiment 1.b. Velocity as a function of the leg angles θ_1 and θ_2.

The individuals reaching a lower velocity either demonstrate a lack of stability due to the leg angles placing the feet under the body, or have shorter legs which do not produce a high velocity.

2) Experiment 1.b: Influence of the leg angles: This experiment's results are a subset of the previous. In order to study the influence of the angles θ_1 and θ_2 on the velocity, the two other parameters that were previously variable are now given a fixed value of $l_1 = l_2 = 0.08$ m.

Figure 8 shows the influence of the θ_1 and θ_2 leg angles on the velocity. One can clearly notice that as expected, $\theta_1 = \theta_2 = 0°$ yields a very bad result, as the feet do not touch the ground and the salamander is incapable of moving forward.

The best individual has the following settings: $\theta_1 = 40°$ and $\theta_2 = 20°$. It demonstrates a velocity of 0.67 m/s. When θ_1 exceeds $50°$, the velocity drops quickly as a consequence of the unstable configurations yielded by these angles. The robot simply falls on its side and crawls chaotically on the ground.

The simulation for these individuals required very short time steps (around 5 ms) in order to avoid numerical explosions caused by the feet violently hitting the ground.

3) Experiment 1.c: Influence of the leg lengths: In this experiment, which also uses a subset of the first experiment's results, the leg angles have been fixed to $\theta_1 = \theta_2 = 30°$. Figure 9 shows how the velocity depends on the leg lengths. As expected, the longest the legs, the highest the velocity.

The best individual is here located at $l_1 = 0.1$ m and $l_2 = 0.08$ m, reaching a velocity of 0.67 m/s.

B. Locomotion controller

In this part we examine the way the robot's performances are affected by modifying the controller's parameters given in the following enumeration. The aim is to identify which waves produce an effective locomotion.

- A: Body servo amplitude. An amplitude of $20°$ means for example that the servo rotates $20°$ in each direction, hence a range of $40°$.

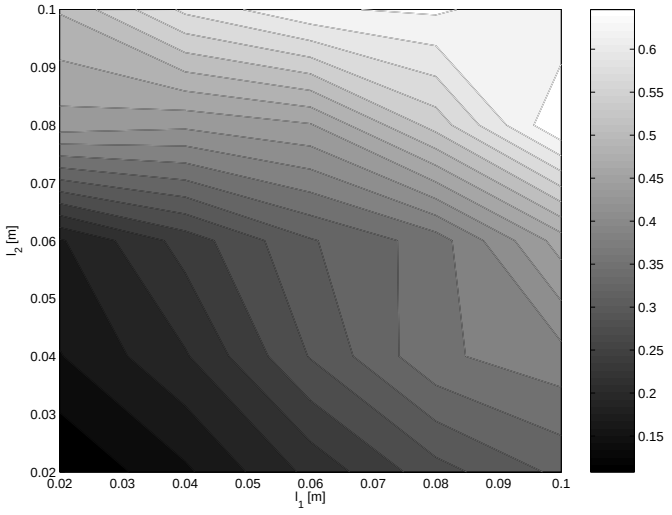

Fig. 9. Experiment 1.c. Velocity as a function of the leg lengths l_1 and l_2.

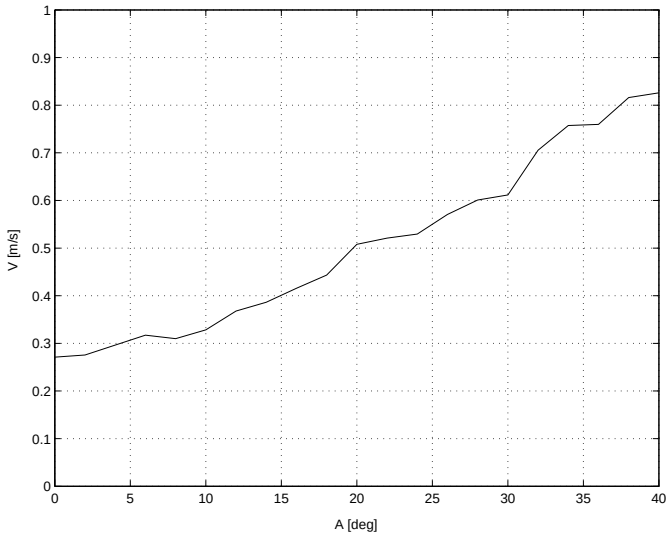

Fig. 10. Experiment 2. Influence of the body undulation in legged locomotion. Velocity as a function of the servo amplitude.

TABLE II

EXPERIMENTS ON THE LOCOMOTION CONTROLLER. VALUES BETWEEN BRACKETS DEFINE THE RANGE AND GRANULARITY: [LOWER-BOUND : STEP : UPPER-BOUND].

Exp number	A [deg]	λ [body length]	ν [Hz]	env	loco
2	[0:2:40]	note†	1	ground	walk
3	[0:3:50]	[0:0.25:5]	1	water	swim
4	[0:1:30]	[0:0.08:5]	[0:0.1:0.5]	water	swim
5	[0:2:50]	[0:0.16:5]	1	ground	crawl
6	[0:1:30]	[0:0.08:5]	[0:0.1:0.5]	ground	crawl

† wavelength as defined in section **??**.

- λ: Body undulation wavelength. For serpentine locomotion it can be set to any value but in case of legged locomotion it is defined by the leg attach position and cannot be arbitrarily chosen.
- ν: Body undulation frequency.
- env: the environment: ground or water.
- loco: the locomotion: walking, swimming or crawling.

Table II shows details about the fixed and variable parameters in each experiment. Since the leg shape of the real robot is not yet defined, the crawling and swimming experiments are done with the legless model.

1) Experiment 2: Influence of the body undulation amplitude in walking: This experiment consists of varying the amplitude of each spine-servo (thus the amplitude of the body undulations) during a legged run, causing the salamander to try all the possibilities, from a constantly straight body to a very pronounced S-shaped body swinging from side to side. That will allow us to examine the way the performances can be enhanced. Figure 10 clearly shows that the body undulations help to augment the overall velocity. A large amplitude produces large steps, therefore the distance covered by each step is also larger. The robot has the following leg settings: $\theta_1 = \theta_2 = 30^\circ$ and $l_1 = l_2 = 0.08$ m.

The velocity reached with a straight body is 0.27 m/s while it is equal to 0.83 m/s with a 40° servo amplitude. The undulation has thus multiplied the velocity by a factor of 3.07.

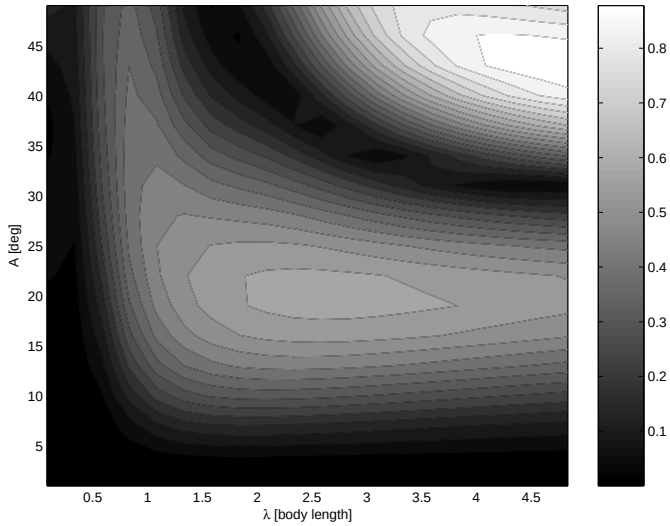

Fig. 11. Experiment 3. Velocity as a function of the body undulation amplitude and wavelength for a swimming snake.

We did not consider amplitudes higher than 40°, because larger bendings of the body tend to induce collisions with the legs.

2) Experiment 3: Influence of the body undulation amplitude and wavelength in swimming: As displayed on figure 11, the augmentation of the oscillation amplitude first causes the velocity to increase up to a particular point, here around 20°, where there is an optimal trade-off between large amplitudes which induce more power in the movements but create S-shaped and less straight trajectories, and small amplitudes creating more 'direct' (straight) trajectories but with less power. The 'valley' running from the top border of the graph to the right one is due to the fact that at a given amplitude, the snake's shape (and trajectory) will resemble an '8' and thus make the robot remain at its original location. Past this point, the performances increase again as the snake starts to swim making loops which, when they unfold, provide a strong thrust to propel the robot. The top right corner of the graph

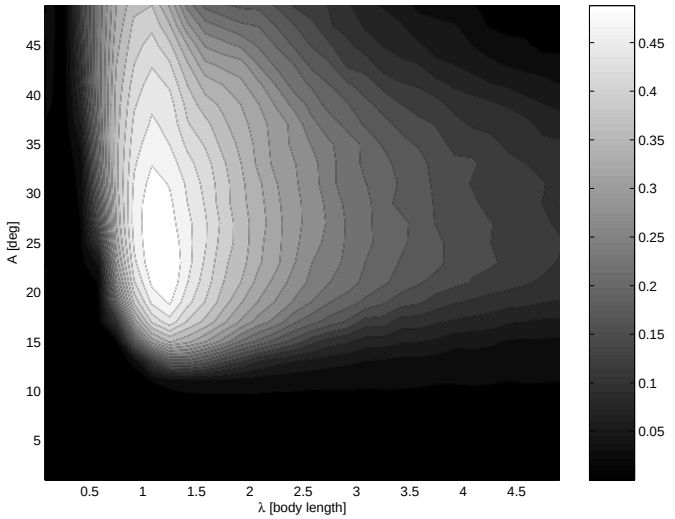

Fig. 12. Experiment 5. Velocity as a function of the body undulation wavelength and amplitude for a crawling snake.

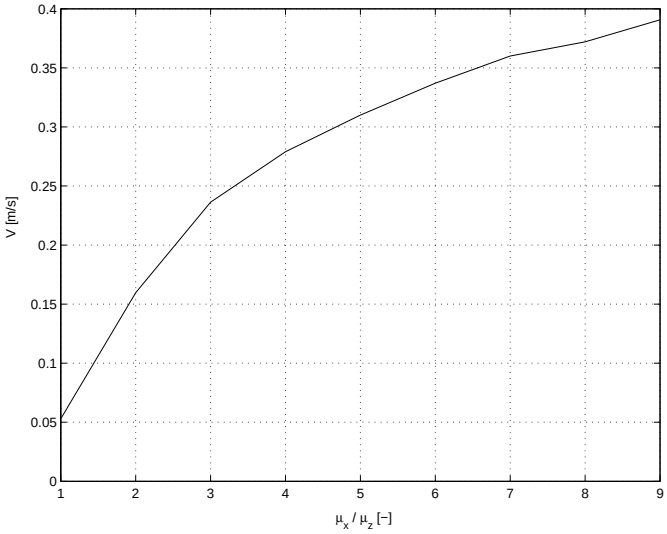

Fig. 13. Experiment 6. Velocity of snakes with servo amplitude and frequency bounded to the realistic values, as a function of the friction ratio.

depicts this effect.

The graph reaches its peak value at $\lambda = 2.6$ body lengths and $A = 20°$. A body wavelength of 2.6 means that the wave described by the body is shorter than an entire cycle, causing the tail to swing from side to side.

3) Experiment 4: The fastest swimmer with parameters bounded to realistic values: We here add the frequency to the search space (i.e. we vary the frequency, amplitude, and wavelength) and explore a search space that is bounded with the limitations of the real robot's servos. The fastest swimmer, has the following optimal settings: $A = 18°$, $\lambda = 2.3$ body lengths and $\nu = 0.5$ Hz. Note that, as might be expected, the optimal solution uses the highest allowed frequency. For such low frequencies the wavelength (above 2 body lengths) has almost no influence on the speed (see also figure 14, left).

4) Experiment 5: Influence of the body undulation wavelength and amplitude in crawling: This experiment is basically the same as experiment 3, except the environment which is in this case the ground. The results are shown on figure 12, with a tangential friction μ_z of 0.1, and a perpendicular friction μ_x of 0.5. The performances seem to decrease much faster when the body wavelength increases as in the swimming motion. This means that the swinging tail motion does not work well on the ground. In water, the snake requires shorter wavelengths and higher frequencies (thus higher relative water velocity) in order to generate the drag forces which in turn will propel the body. This is a consequence of the drag forces being proportional to the squared velocity, hence low speeds will produce very low drag. In the contrary, the asymmetric friction of the snake's body on the ground can act even by very low speeds.

5) Experiment 6: The fastest snake with parameters bounded to the realistic values: This experiment is similar to experiment 4, except that it happens on the ground. There is however another difference: the friction coefficients μ_x and μ_z between the ground and the body, which allow crawling, are still unknown, furthermore they can take different values depending on the properties of the ground and robot surfaces.

TABLE III

EXPERIMENT 6. OPTIMAL SETTINGS FOR A SNAKE ON THE GROUND FOR DIFFERENT VALUES OF THE FRICTION RATIO μ_r AND PARAMETERS BOUNDED TO REALISTIC VALUES

μ_r [-]	A [deg]	λ [body length]	ν [Hz]	V [m/s]
1	30	1.0	0.5	0.05
2	30	1.2	0.5	0.16
3	28	1.3	0.5	0.24
4	24	1.5	0.5	0.28
5	22	1.7	0.5	0.31
6	20	1.7	0.5	0.34
7	20	1.8	0.5	0.36
8	20	2.2	0.5	0.37
9	20	2.0	0.5	0.39

The question is now: How does the ratio $\mu_r = \mu_x/\mu_z$ affect the velocity? The answer should give an idea of the importance of the materials or the device (e.g. rubber wheels which can easily simulate a high μ_r) needed to produce the friction. Figure 13 shows the speeds (computed from 30 s runs) of the best individuals with $A \leq 30°$ and $\nu \leq 0.5$ Hz. It represents, for each μ_r, the velocity of the fastest individual. The longitudinal friction coefficient μ_z has been set to 0.1 for all runs and the transversal one, μ_x, ranges from 0.1 to 0.9. The good surprise is that the curve is bent upward, it means that even low friction ratios can yield fair velocities. For instance, to achieve half of the average speed of the best individual with $\mu_r = 9$, you do not need $\mu_r/2$ but a lower value ($\approx \mu_r/3.6$) which is easier to obtain than $\mu_r/2$.

These 'best individuals' cited above all have different optimal amplitudes and wavelengths, provided in table III: According to the experiment, the friction ratio μ_r should be as high as possible and the frequency as well. The amplitude and wavelength should then be adapted depending on the value of μ_r to provide a maximal velocity.

From this table, we can deduce the limiting factors. The frequency is in every case equal to the upper limit, 0.5 Hz. Moreover, for friction ratios under 3, the amplitude also

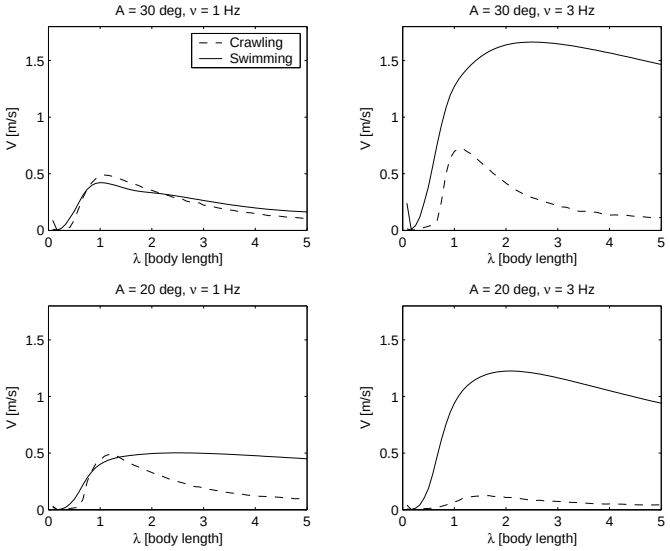

Fig. 14. Influence of the body wavelength in terrestrial (dashed line) and aquatic (full line) locomotion.

becomes a limiting factor.

6) Comparison of optimal wavelengths in swimming and serpentine locomotion: We have roughly seen that the optimal frequencies, wavelengths and amplitudes differ depending on the environment. In order to provide a better view of the differences, comparative runs can be conducted. By fixing the amplitude and the frequency we can compare the effect of the body wavelength on the velocity and by repeating the operation with different settings, the trend can be guessed. The friction ratio μ_r is here fixed to 5. Figure 14 shows the performances for the same individual on the ground and in the water. As previously seen, the terrestrial locomotion has a narrow peak around the optimal wavelength whereas the aquatic motion does not especially suffer from high λ's. This behavior can be seen in nature, e.g. fish swinging their tail from side to side by bending their body in one way only (long wavelength), contrary to real snakes undulating by creating numerous bendings (short wavelength).

We can also notice that swimming can reach much higher speeds, provided the frequency is over 1 Hz (which is unfortunately above the upper limit for our real robot's servos). This result matches studies performed on real sea-snakes, which demonstrates that swimming is faster than crawling [25]. This all shows that a modification of the undulation is recommended when passing from earth to water.

VI. Discussion

Experiments showed that during legged locomotion, in order to maximize the velocity, the circle described by the feet spinning should be as far as possible from the body with a radius as large as possible. That means that long legs produce higher velocity, provided the stability is assured. Long femurs seem to have a stabilizing effect when the leg angles are set to a reasonable value. Slightly changing the orientation of the leg rotation axes[2] can be beneficial but it should remain in the horizontal plan to avoid instabilities. Body undulations help to augment the velocity but, exceeding some value, they increase the risk of leg-to-leg or leg-to-body collisions.

When swimming, the optimal body wavelength appears to be over 2 body lengths in which case the tail swings from side to side with a C-shaped undulation the same way some fishes do. The optimal frequency, body amplitude and wavelength for swimming have been determined for a 12-segments swimming snake with the frequency and amplitude bounded to values corresponding to the real robot's limits.

It appears that in water, contrary to the motion on ground, a slow motion will hardly produce a forward movement as the 'propelling forces' are proportional to the squared relative velocity. In crawling, the optimal wavelengths are generally shorter than in the water, to avoid, among other phenomena, a swinging tail which is not adapted to this terrestrial type of locomotion. The optimal wavelength and amplitude depends on the friction properties of the ground.

Simulations with different transversal-to-longitudinal friction ratios (which allow serpentine locomotion) have shown that the higher it is, the faster the snake becomes. However, the augmentation of velocity does not grow linearly as the ratio increases; it grows faster for low ratios.

The real servo's top frequency of 0.5 Hz is in most of the cases a limiting factor. Faster servos would greatly improve the salamander's velocity. It would naturally have an effect on the power consumption.

The simulated salamander robot performs realistic motions, in the three different types of locomotion we tested. However, a fair number of variables and coefficients have been rather arbitrarily set, since the exact value they shall take is still unknown. The determination of these values will precisely be one of the tasks to be done when the real robot's assembly will be achieved. Among these unknown parameters are: the friction coefficient between the robot and the ground, the mass and volume of the robot's segments (which will determine the density), the center of gravity's (CG) exact position.

Some other parameters have been approximated, like for instance all the drag coefficients, the external forces simulating the effects of water. The computation of the immersed volume for Archimedes' force is an approximation when the salamander is only partially immersed, the drag force's computation is also an approximation since it is in our case a vectorial summation of forces separately computed along each axis. Moreover, as all body segments are considered to be two-dimensional (in terms of fluids mechanics), the first and the last segments are slightly farther away from reality than the mid-body segments since the former have only one neighbor thus allow the water flow to pass around one of their sides. Similarly, when the body is only partially immersed, The drag forces are computed just as in the completely-immersed case. The motion of the water itself is not modeled. There are no turbulences and vortexes in the simulation.

Nevertheless, since every instance of the salamander model suffered from the same approximations, we expect that comparative tests (which were the core of the present work) are still valid and provide relevant information. Experiments with the real robot will allow us to verify the quality of the simulation.

[2]Experiment not shown in this article.

VII. Future Work

a) Power consumption: The optimization of the power consumption is an important issue, which directly influences the robots mobility by reducing or extending its 'lifetime'. Furthermore, some fast gaits may be very inefficient, i.e. consuming much power.

b) 2D locomotion: The ability to turn left and right, must definitely be studied, by taking into account the body's dynamics. Performing a turn can be simply done by adding an offset value to each body servo's α_i angle. A positive offset will make the robot turn right and a negative one will make it go left (it may be reversed, depending on the servo's orientation). Early test runs performed during this work have demonstrated a very good behavior for turning in serpentine locomotion (both on the ground or in the water). Turning while walking was however more difficult to achieve because it requires an adapted coordination between the limbs. A user interface was created for a direct direction control of the robot.

Attitude modification around the pitch and roll axes when swimming can be performed by modifying the orientation of the legs (using them as rudders) and has been successfully tested.

c) Transitions between ground and water: Transiting from one element to the other, one of the key points in amphibious locomotion, must be carefully planned as it is a critical stage. Even the best swimmer *and* walker would make a poor amphibious robot if it is unable to crawl out of the water. The parameters that must be tested are for example the strategy for detecting water, the timing of locomotion transition or the potential use of an 'intermediate' gait (e.g. front legs rotating while rear legs and tail still in a swimming mode).

d) Crossing: Crossing capabilities (passing over an obstacle or climbing a step) have not yet been addressed but shall be one of the determining criteria in the search for the optimal leg and body configuration. Climbing is precisely one of the advantages of legged locomotion and motivates its choice. The current robot will have problems due to the planar configuration of its spine. The simulation can be used to identify how many additional degrees of freedom can be added to the spine to allow bendings in the vertical plane.

e) Comparison with the real robot: Comparing the simulated model with the real robot will allow us to tune the model's settings in order to get closer to reality. The model currently used to simulate water could also be enhanced (empirically) to become more realistic, for example the effect of water motion, waves generated by the robot, etc. Comparative test runs should be performed in parallel, in the real world and in the simulator.

f) Genetic Algorithms: Because of the very large search space and the correlation between all the parameters, the most suitable tool to reach an optimum is probably the genetic algorithm — optimization through evolution and selection, survival of the best individuals. The parameters that should play a role in the fitness function are the velocity (or distance between the start and final positions, both on the ground or in the water), the time of velocity stabilization, the crossing capabilities, the power consumption, the stability, the ability to crawl out of the water, etc. The use of a genetic algorithm for optimization will become relevant only when all parameters have been correctly set in the simulation to match reality.

VIII. Conclusion

A software model of the salamander has been created in the Webots robot simulator. The salamander can demonstrate walking, swimming and crawling locomotion. A program allowing the generation of custom-shaped salamanders (with or without legs, different dimensions, lengths, angles and controller settings) was developed as well. The robot software model and Webots both require some additional refinements to obtain a high-fidelity simulation and prediction tool, but the versions used in the present work were accurate enough to provide useful informative and comparative data. Test runs were performed in order to explore the characteristics of the salamander robot's locomotion using the three different motions, walking, crawling and swimming. The influences of the different morphology and movement parameters on the velocity were analyzed.

The present work has paved the way for later work aiming at defining the salamander robot's definitive morphology and controller. It has provided a research tool for optimization process to be conducted (e.g. genetic algorithms) in order to reach that goal.

References

[1] A. Crespi, A. Badertscher, A. Guignard, and A. Ijspeert, "An amphibious robot capable of snake and lamprey-like locomotion," in *ISR 2004*, 2004.

[2] ——, "AmphiBot I: an amphibious snake-like robot," 2004, in preparation.

[3] M. Raibert and J. Hodgins, "Legged robots," in *Biological Neural Networks in Invertebrate Neuroethology and Robotics*, R. Beer, R. Ritzmann, and T. McKenna, Eds. Academic Press, 1993, pp. 319–354.

[4] M. Fujita and K. Kageyama, "An open architecture for robot entertainment," in *Proceedings of the First International Conference on Autonomous Agents, Marina del Rey, CA*, 1997, pp. 435–442.

[5] Y. Fukuoka, H. Kimura, and A. Cohen, "Adaptive dynamic walking of a quadruped robot on irregular terrain based on biological concepts," *The International Journal of Robotics Research*, vol. 3–4, pp. 187–202, 2003.

[6] M. Lewis, "Self-organization of locomotory controllers in robots and animals," Ph.D. dissertation, Faculty of the Graduate School, University of Southern California, August 1996.

[7] R. Breithaupt, J. J. Dahnke, J. Hertzberg, and F. Pasemann, "Robot-salamander - an approach for the benefi t of both robotics and biology," in *Fifth International Conference on Climbing and Walking Robots (CLAWAR-2002)*, P. B. (Ed), Ed., 2002, pp. 55–62.

[8] A. Hiraoka and H. Kimura, "A development of a salamander robot - design of a coupled neuro-musculoskeletal system -," in *Proceedings of Annual Conf. of RSJ, 2H12, Osaka*, 2002, in Japanese.

[9] S. Hirose, *Biologically Inspired Robots (Snake-like Locomotor and Manipulator)*. Oxford University Press, 1993.

[10] G. Miller, *Neurotechnology for biomimetic robots*. Bradford/MIT Press, Cambridge London, 2002, ch. Snake robots for search and rescue.

[11] K. Paap, M. Dehlwisch, and B. Klaassen, "GMD-snake: a semi-autonomous snake-like robot," in *Distributed Autonomous Robotic Systems 2*. Springer-Verlag, 1996.

[12] D. Mihalachi, "Système de commande temps réel distribué pour un mini robot autonome de type serpent," Ph.D. dissertation, Université de Metz, 2000.

[13] J. Ayers, C. Wilbur, and C. Olcott, "Lamprey robots," in *Proceedings of the International Symposium on Aqua Biomechanisms*. Tokai University, 2000.

[14] K. McIsaac and J. Ostrowski, "A geometric approach to anguilliform locomotion: Modelling of an underwater eel robot," in *Proceedings of the 1999 IEEE Conference of Robotics and Automation (ICRA1999)*, 2001, pp. 2843–2848.

[15] M. Triantafyllou and G. Triantafyllou, "An effi cient swimming machine," *Scientific American*, vol. 272, no. 3, pp. 40–48, 1995.
[16] J. Anderson and P. Kerrebrock, "The vorticity control unmanned undersea vehicle (VCUUV) - an autonomous vehicle employing fi sh swimming propulsion and maneuvering," in *Proc. of the Autonomous Undersea System Institute 10th International Symposium on Unmanned Untethered Submersible Technology*, 1997, pp. 189–195.
[17] R. Altendorfer, N. Moore, H. Komsuoglu, M. Buehler, H. Brown Jr., D. McMordie, U. Saranli, R. Full, and D. Koditschek, "RHex: A biologically inspired hexapod runner," *Autonomous Robots*, vol. 11, p. 207, 2001.
[18] J. Ayers, J. Witting, N. McGruer, C. Olcott, and D. Massa, "Lobster robots," in *Proceedings of the International Symposium on Aqua Biomechanisms*. Tokai University, 2000.
[19] T. Takayama and S. Hirose, "Development of helix: a hermetic 3d active cord with novel spiral swimming motion," in *Proceedings of TITech COE/Super Mechano-Systems Symposium*, 2001.
[20] I. Delvolvé, T. Bem, and J.-M. Cabelguen, "Epaxial and limb muscle activity during swimming and terrestrial stepping in the adult newt, *Pleurodeles Waltl*," *Journal of Neurophysiology*, vol. 78, pp. 638–650, 1997.
[21] A. Ijspeert, "A connectionist central pattern generator for the aquatic and terrestrial gaits of a simulated salamander,," *Biological Cybernetics*, vol. 84, no. 5, pp. 331–348, 2001. [Online]. Available: http://birg.epfl.ch/page27911.html
[22] O. Michel, "Webots: Professional mobile robot simulation," *Journal of Advanced Robotics Systems*, vol. 1, no. 1, pp. 39–42, 2004. [Online]. Available: http://www.ars-journal.com/ars/Volume1Number1/39-42.pdf
[23] Open Dynamics Engine ODE, Library for simulating articulated rigid body dynamics. [Online]. Available: http://ode.org/
[24] F. White, *Fluids Mechanics*, 4th ed. WCB/McGraw-Hill, pp. 458–460.
[25] R. Shine, H. Cogger, R. Reed, S. Shetty, and X. Bonnet, "Aquatic and terrestrial locomotor speeds of amphibious sea-snakes (Serpentes, Laticaudae)," *Journal of Zoology*, vol. 259, pp. 261–268, 2003.
[26] J. Collins and S. Richmond, "Hard-wired central pattern generators for quadrupedal locomotion," *Biological Cybernetics*, vol. 71, no. 5, pp. 375–385, 1994.

Jérôme Braure Biography text here.

Olivier Michel Biography text here.

Alessandro Crespi Biography text here.

Auke Jan Ijspeert Biography text here.